

SPECTROSCOPIC PROPERTIES OF RARE EARTH BOROHYDRIDES: $\text{Er}(\text{BH}_4)_3 \cdot 3\text{THF}$ IN PURE AND MIXED CRYSTALS*

E.R. BERNSTEIN** and K.M. CHEN †

Princeton University, Department of Chemistry, Princeton, N.J. 08540, USA

Received 4 June 1975

The optical spectra of $\text{Er}(\text{BH}_4)_3 \cdot 3\text{THF}$ neat crystals and La, Gd, $\text{Y}(\text{BH}_4)_3 \cdot 3\text{THF}$ mixed crystals are reported and analyzed. Lanthanum borohydride is found to have a different room temperature crystal structure (triclinic) from Er, Gd, $\text{Y}(\text{BH}_4)_3 \cdot 3\text{THF}$ (Pbcn). At low temperature the Pbcn crystals undergo a phase transition to a structure with two crystallographically inequivalent sites in a unit cell. The optical spectra of $\text{Er}(\text{BH}_4)_3 \cdot 3\text{THF}$ in Er, Y, Gd $(\text{BH}_4)_3 \cdot 3\text{THF}$ crystals clearly evidence these two sites. Large vibronic intensity is observed at 1.6 K and 77 K and nine "molecular" vibrations are assigned. These modes are quite similar to those found for $\text{U}(\text{BH}_4)_4$. $\text{Er}(\text{BH}_4)_3 \cdot 3\text{THF}/\text{La}(\text{BH}_4)_3 \cdot 3\text{THF}$ spectra are very different: no vibronic transitions are observed but many (often upwards of fifty for a given manifold) weak sharp "satellite" lines are found associated with pure electronic transitions. These data are discussed in terms of structural differences and comments on bonding and covalent character in lanthanide borohydrides are made.

1. Introduction

The electronic transitions of lanthanide ($4f^n$) solids are well characterized by a weak crystal field theory and these ions serve as excellent probes of crystal interactions and symmetry. The theory of rare earth ion energy levels and many confirming experimental observations are now available [1]. However, the range of chemistry of this f-electron series has only recently been explored. Most lanthanide compounds are highly ionic in nature. Over the last twenty years, however, an organo-metallic chemistry of this transition series has begun to develop [2]. Notably, cyclopentadienides (cpd), indenides, cyclooctatetraenides, and phenyl compounds have been synthesized. Structural studies [3–7] are available for a number of rare earth organometallics and spectra have been observed for a variety of $\text{Ln}(\text{cpd})_3$ systems [8–14].

The crystal structure of $\text{Sm}(\text{cpd})_3$ has been reported to be rather complex with two crystallographically inequivalent sites in a unit cell [6]. $\text{Sc}(\text{cpd})_3$ has been reported to have a different structure with only one type of site per unit cell [4]. Both structures are polymeric in nature with four cpd groups arranged around each metal ion. Optical spectra of $\text{Er}(\text{cpd})_3$ evidences large crystal field splittings and some vibronic intensity [10,14,15]; nonetheless those compounds are described as largely ionic (less than 3% covalency) [8]. These studies have begun to deal with the general problems of bonding, structure, and chemistry in the lanthanide series.

The borohydride ligand (BH_4) has been shown to give covalent compounds in the actinide and other transition metal series [16]. It would appear from structural data on actinide borohydrides $\text{M}(\text{BH}_4)_4$, that there is a possibility for f-orbital participation in the hydrogen bridge bonding [17,18]. With these facts as motivation, rare earth borohydrides have been synthesized and studied structurally and spectroscopically. Erbium was chosen as the ion to be investigated first, after some initial work with neodymium, because its large spin-orbit coupling makes for well separated f -manifolds.

* Work supported, in part, by ONR, ARO-D, NSF, and the Research Corporation.

** Present address: Department of Chemistry, Colorado State University, Fort Collins, Colorado 80523.

† Present address: Department of Chemistry, Iowa State University, Ames, Iowa 50010.

In this initial report on the spectroscopic properties of lanthanide borohydrides we discuss spectra of $\text{Er}(\text{BH}_4)_3 \cdot 3\text{THF}$ neat crystals and mixed crystals of $\text{Er}(\text{BH}_4)_3 \cdot 3\text{THF}$ in La , Gd , $\text{Y}(\text{BH}_4)_3 \cdot 3\text{THF}$. These spectra show large but not extraordinary crystal field splitting and, with the exception of $\text{Er/La}(\text{BH}_4)_3 \cdot 3\text{THF}$, give very substantial sharp vibronic intensity. In some J -manifolds the vibronic intensity is as much as an order of magnitude larger than the pure electronic intensity. Observed vibrational frequencies are those expected for transition metal borohydrides based on Th , U , Zr , $\text{Hf}(\text{BH}_4)_4$ values [16,18,19]. They are also consistent with infrared and Raman spectra of $\text{Gd}(\text{BH}_4)_3 \cdot 3\text{THF}$ crystals obtained in our laboratory [20].

Structural studies on these crystals, presently in progress [21], have proven quite interesting. The room temperature structures of Er , Y , $\text{Gd}(\text{BH}_4)_3 \cdot 3\text{THF}$ are isomorphic having space group Pbcn with four molecules per unit cell. The rare earth ions are at sites of C_2 symmetry. At lower temperatures ($250 \geq T_c \geq 77 \text{ K}$) these crystal undergo a phase transition such that each unit cell of the new space group contains two crystallographically inequivalent (distinct) sites. $\text{La}(\text{BH}_4)_3 \cdot 3\text{THF}$ has a room temperature triclinic space group (most likely P1). It is not known if this crystal undergoes a phase transition at some lower temperature. The optical spectra are consistent with these structural differences and are the source of the assigned low temperature phase change in Er , Y , $\text{Gd}(\text{BH}_4)_3 \cdot 3\text{THF}$. Infrared and Raman room temperature data indicate a covalency in these systems more like Th , $\text{U}(\text{BH}_4)_4$ than NaBH_4 [18–20], suggestive of mixed two- and three-hydrogen bridged borohydride groups in a polymeric array [17].

In the following section we discuss synthesis, crystal growth, crystal mounting, and spectroscopic techniques. In section 3 results of these studies are presented and in section 4 the data are discussed and correlated.

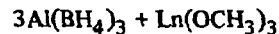
2. Experimental

2.1. Synthesis of $\text{Ln}(\text{BH}_4)_3 \cdot 3\text{THF}$

All rare earth borohydrides can be synthesized by either of two routes. The crystalline product of either

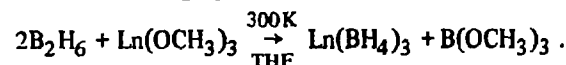
method gives an analyzed ratio of one rare earth ion (La , Nd , Gd , Er , and Y), to three tetrahydroborate groups (BH_4), to three coordinated molecules of tetrahydrofuran (THF , $\text{C}_4\text{H}_8\text{O}$). Previous attempts to obtain these compounds [22] generally yielded non-integer ratios of coordinated THF . Since borohydrides are air sensitive, greaseless high vacuum techniques were employed throughout.

The first method used to obtain $\text{Ln}(\text{BH}_4)_3$ gives the overall reaction (60% yield):



The $\text{Al}(\text{BH}_4)_3$ [23a] and $\text{Ln}(\text{OCH}_3)_3$ [23b] were obtained by standard methods. No crystals could be obtained except when $\text{Ln}(\text{BH}_4)_3$ was dissolved in THF . However, in order to isolate the desired $\text{Ln}(\text{BH}_4)_3$, unreacted $\text{Al}(\text{BH}_4)_3$ and other aluminium reaction and decomposition products had to be removed by distillation and sublimation. The reaction mixture was then washed with cyclohexane and benzene, in which $\text{Ln}(\text{BH}_4)_3$ are insoluble, for the final purification step.

The method by which pure product and crystals can be readily obtained is reaction of $\text{Ln}(\text{OCH}_3)_3$ with diborane B_2H_6 in a THF solution (~100% yield).



THF and $\text{B}(\text{OCH}_3)_3$ are pumped off and product is washed with fresh THF and vacuum filtered. B_2H_6 is purchased from Callary Chemical Co. (Callary, Pa.) and extensively vacuum sublimed and distilled before use, rare earth metal oxides (99.99% pure) are purchased from American Potash and Chemical Co., Rare Earth Division (West Chicago, Illinois), LnCl_3 (used for $\text{Ln}(\text{OCH}_3)_3$ preparation) were synthesized by standard techniques [23c], and all solvents were purified by standard methods. A very detailed and complete description of these procedures is available [24].

2.2. Crystal growth

Large single crystals of all the lanthanide borohydrides can be grown from THF but not di-ethyl ether or methyl- THF solution. While these latter two solvents will give quantitative synthetic yields, only glasses could be obtained by cooling them. Saturated

THF solutions of the lanthanide or mixtures of lanthanides were vacuum transferred into a flask glass blown onto a quartz sample cell. The shape of this crystal grower was that of an inverted "U". The apparatus was filled with 200–600 torr of helium gas. A seed crystal was obtained and worked into position in the optical cell. The initial growth procedure was to slowly lower the temperature of this saturated solution (ca. 30°C) to ambient temperature over about a two week period. THF was then slowly distilled (2 to 6 weeks) out of the thermostated sample cell. When the crystal was of sufficient size, THF was drained away and the cell glass blown off the apparatus. Such crystals were invariably single but of random orientation. All crystals are optically biaxial.

2.3. X-ray crystals

Crystals of $\text{La}(\text{BH}_4)_3 \cdot 3\text{THF}$, $\text{Y}(\text{BH}_4)_3 \cdot 3\text{THF}$, and $\text{Gd}(\text{BH}_4)_3 \cdot 3\text{THF}$ were mounted for X-ray study in 0.3 mm \times 4 cm quartz capillary tubes. It proved quite difficult to mount air sensitive crystals (0.1 \times 0.25 \times 0.4 mm) that tend to decompose with no solvent present. It was found that crystals could be mounted without solvent in the X-ray capillary tubes (preferable because small temperature changes either float crystals or cause more material to precipitate out on the chosen crystal) if they were handled in a glove bag whose atmosphere was saturated with dry THF. Samples were sealed in capillaries with a torch. Details of the X-ray data collection can be found elsewhere [17a,21].

2.4. Susceptibility measurements

Magnetic measurements on powdered $\text{Er}(\text{BH}_4)_3 \cdot 3\text{THF}$ were performed at Bell Laboratories by Dr. F.J. DiSalvo. The techniques and apparatus are discussed in detail elsewhere [25]. Crystals were crushed in a glove bag to get powders and were handled in a similar fashion to X-ray samples.

2.5. Optical spectroscopy

Low temperature optical spectra were obtained at medium resolution. Spectra were taken photographically on a 2m Czerny–Turner spectrograph with a 1200 groove/mm grating, blazed at 7500 Å. This com-

bination gives a 3.6 Å/mm first order dispersion at the exit plane. Slit widths ranged from 25 to 40 μm . Kodak 103a-O, F and I–N plates were used in the appropriate spectral regions. All lines reported are accurate to $\pm 0.5 \text{ cm}^{-1}$ which is about three standard deviations for the sharper lines. Wave length calibration was achieved with hollow cathode iron–neon lamps. Spectra were taken with tungsten filament and high pressure xenon (Hanovia 959c-198) lamps. Samples were cooled slowly to 77 K over a period of a few days. Cells were loaded with 600 torr of helium at 300 K in an attempt to increase thermal conductivity to the bath. At a bath temperature of roughly 1.6 K, samples could be heated to probably about 5 K judged from hot band intensity.

3. Results

3.1. Crystal structure

The room temperature crystal structure studies of $\text{Ln}(\text{BH}_4)_3 \cdot 3\text{THF}$ are still in progress [21] but certain features of these structures are known and are relevant to the present spectroscopic investigations. $\text{Gd}(\text{BH}_4)_3 \cdot 3\text{THF}$, $\text{Y}(\text{BH}_4)_3 \cdot 3\text{THF}$, and $\text{Er}(\text{BH}_4)_3 \cdot 3\text{THF}$ (the latter by spectroscopic inference) all have the same room temperature orthorhombic space group D_{2h}^{14} (Pbcn). The unit cell dimensions for $\text{Gd}(\text{BH}_4)_3 \cdot 3\text{THF}$ are, $a = 9.28 \text{ \AA}$, $b = 14.52 \text{ \AA}$ and $c = 14.53 \text{ \AA}$, and for $\text{Y}(\text{BH}_4)_3 \cdot 3\text{THF}$ they are $a = 9.26 \text{ \AA}$, $b = 14.49 \text{ \AA}$, and $c = 14.43 \text{ \AA}$. Errors at this stage of refinement are probably $\pm 0.02 \text{ \AA}$. The number of molecules in the unit cell for both crystals is four and the metal ions are at sites of 2-fold symmetry.

$\text{La}(\text{BH}_4)_3 \cdot 3\text{THF}$ is triclinic at this temperature with the most likely space group being P1. The rare earth ion in this structure occupies a general position.

3.2. Susceptibility

The magnetic susceptibility of $\text{Er}(\text{BH}_4)_3 \cdot 3\text{THF}$ indicates that between 310 and 4.2 K there is no magnetic phase transition; based on a χ_g (magnetic susceptibility per gram, emu/g) versus $1/T(\text{K}^{-1})$ plot, neat crystals follow a Curie law and are paramagnetic. The effective high temperature moment over this range is $\mu_{\text{eff}} = 8.83 \text{ BM}$, and the low temperature slope gives

$\mu_{\text{eff}} = 5.16$ BM. The low temperature value corresponds to a $|\bar{g}|$ (average effective g -value) of 5.96 for a $J' = \frac{1}{2}$ level. An excited ground manifold level can be observed at about 12 cm^{-1} .

3.3. Optical spectra

Data have been collected for neat $\text{Er}(\text{BH}_4)_3 \cdot 3\text{THF}$ crystals (1 and 2 mm path lengths), 1% $\text{Er}^{+3}/\text{Y}(\text{BH}_4)_3 \cdot 3\text{THF}$ crystals (16 mm path length), 5% $\text{Er}^{+3}/\text{Gd}(\text{BH}_4)_3 \cdot 3\text{THF}$ crystals (6 and 8 mm path lengths), and 1%, 5%, 20% $\text{Er}^{+3}/\text{La}(\text{BH}_4)_3 \cdot 3\text{THF}$ crystals. Of the possible 41 J -manifolds in the $f^3(f^{11})$ configuration, 13 have been observed in absorption from the $4I_{15/2}$ ground state. The amount of spectroscopic data is overwhelming and it would serve no useful purpose to report it all in this paper. We have thus chosen to summarize, in figures and a few tables, the most representative and important aspects of this study. Complete listings of all observed transitions can be obtained upon request [24].

Spectra for $\text{Er}(\text{BH}_4)_3 \cdot 3\text{THF}$ pure crystal and Er^{+3}/Gd , $\text{Y}(\text{BH}_4)_3 \cdot 3\text{THF}$ are virtually identical for electronic origins ($\pm 1.0 \text{ cm}^{-1}$) and within $\pm 2.0 \text{ cm}^{-1}$ for vibronic bands. Figs. 1 through 6 show examples of these spectra at 77 and 1.6 K. Electronic origins are listed in table 1 and vibronic transitions are indicated as vibrations observed for various manifolds in table 2. The figures are intended to present an accurate picture of relative electronic and vibronic intensity in each J -manifold.

For $\text{Er}^{+3}/\text{La}(\text{BH}_4)_3 \cdot 3\text{THF}$ again only electronic origins are tabulated (table 1). While there is little or no vibronic intensity for these samples, there are many weak features whose intensity is related (but not quadratically) to Er^{+3} concentration. In some J -manifolds (e.g., $4G_{11/2}$), the number of satellite transitions is upwards of fifty. The energy of these lines is consistent from sample to sample but their intensity also varies with crystal optical quality. Figs. 7 and 8 give a reasonable representation of these features.

From spectra taken at 77 K it is possible to obtain information on the ground electronic manifold and its vibrational states. Table 3 summarizes this data.

4. Discussion

The general theory of spectroscopic properties of

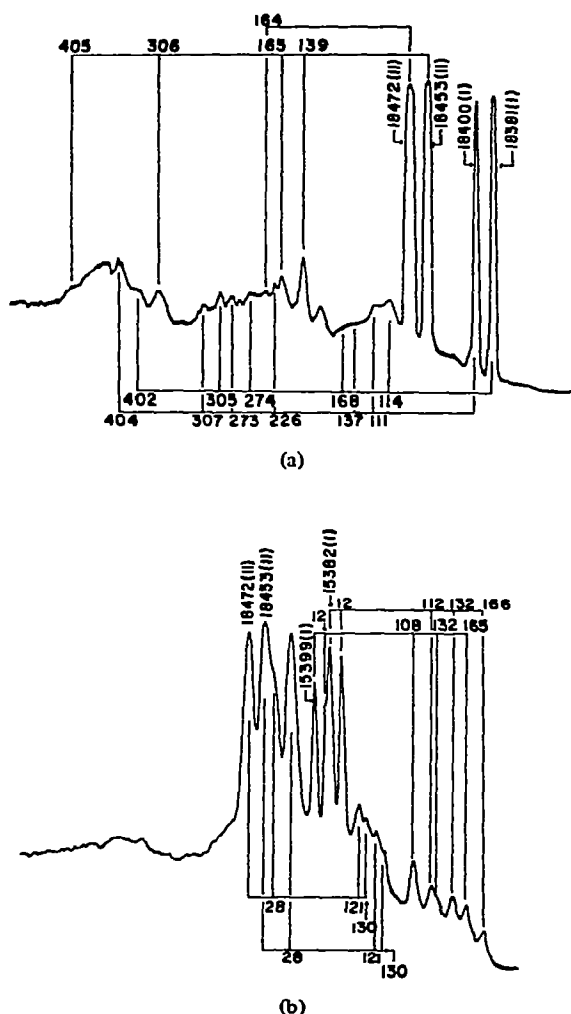


Fig. 1. Absorption spectra of pure $\text{Er}(\text{BH}_4)_3 \cdot 3\text{THF}$ $4S_{3/2}$ manifold. Electronic origins are indicated by their transition frequency (cm^{-1}) and site system (I or II). Vibronic features are connected to their associated electronic origins and assigned vibrational frequencies (cm^{-1}) are given. The vertical scale is arbitrary absorbance: a) 1.6 K; b) 77 K. Hot bands are indicated by energy (cm^{-1}). For site I lines, 12, 108, 132, 165 cm^{-1} hot bands can be assigned; for site II lines, 28, 121, 130 cm^{-1} hot bands are assigned. See table 3 for ground manifold structure.

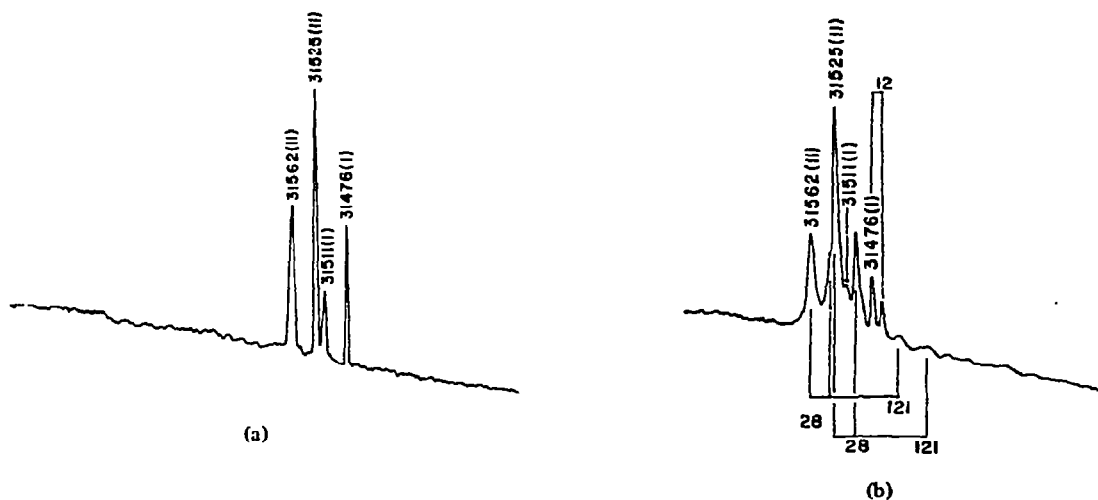


Fig. 2. (a) Absorption spectrum of pure $\text{Er}(\text{BH}_4)_3 \cdot 3\text{THF } ^2\text{P}_{3/2}$ manifold at 1.6 K. Electronic origins are indicated by their transition frequency (cm^{-1}) and site system (I or II). This is the only manifold with very low intensity vibronic features. The two sites structure can be recognized easily from this simple manifold. (b) Absorption spectrum of pure $\text{Er}(\text{BH}_4)_3 \cdot 3\text{THF } ^2\text{P}_{3/2}$ manifold at 77 K. For site I lines, a 12 cm^{-1} hot band is identified. For site II lines, 28 and 121 cm^{-1} hot bands are identified.

rare earth ions (RE^{+3}) is readily applicable to $\text{Er}^{+3}(f^{11})$ in $\text{Er}(\text{BH}_4)_3 \cdot 3\text{THF}$ [1]. The J -manifolds are reproduced from crystal data using three Racah parameters $E^1 \approx 6700 \text{ cm}^{-1}$, $E^2 \approx 32 \text{ cm}^{-1}$, and $E^3 \approx 650 \text{ cm}^{-1}$ and a spin-orbit coupling constant $\zeta \approx 2360 \text{ cm}^{-1}$. The crystal field is assumed only to split each individual "free-ion" J -manifold with little mixing of these manifolds. The number of "Stark" levels for a given J -manifold in a low symmetry crystal field is, due to Kramers degeneracy for odd electron systems, $\frac{1}{2}(2J+1)$ or $(J+\frac{1}{2})$. Comparison of the centers of gravity of J -manifolds of many different systems (i.e., Er^{+3}/Gd , Er , Y , $\text{La}(\text{BH}_4)_3 \cdot 3\text{THF}$, $\text{Er}(\text{cpd})_3$, $\text{Er}^{+3}/\text{LaCl}_3$, $\text{La}(\text{C}_2\text{H}_5\text{SO}_4)_3 \cdot 9\text{H}_2\text{O}$, Y_2O_3 , etc.) relative to the ground level of the lowest J -manifold ($^4I_{15/2}$) reveals this is clearly an adequate approach, in general. If complete data on all manifolds, including the ground manifold, are available, mixing of free ion manifolds by the crystal and configuration interactions does lead to better data fits. For a crystal field symmetry of C_2 or lower (the present situation) a crystal field parameter fit would involve 15 or 27 (C_2 or C_1 sites) total parameters. While there is sufficient data for such an exercise it does not seem useful (that is, it would add

little physical insight) under the circumstances. When a complete crystal structure analysis becomes available it may be possible to model the actual site by some higher crystal field symmetry, such as trigonal or tetragonal. It would then be quite informative to carry out an approximate crystal field analysis.

4.1. The neat crystal and Gd , $\text{Y}(\text{BH}_4)_3 \cdot 3\text{THF}$ mixed crystals

These three systems are discussed as a unit because their low temperature spectra are, to $\pm 1.0 \text{ cm}^{-1}$, superimposable and their crystals possess the same room temperature structure. What is abundantly obvious, from just a cursory look at the simple manifolds ($^4\text{S}_{3/2}$, $^4\text{F}_{3/2}$, $^4\text{P}_{3/2}$, see figs. 1 and 2 and table 1), is that there are twice as many electronic origins as there should be based on the $(J+\frac{1}{2})$ rule. While it is possible that the neat and $\text{Gd}(\text{BH}_4)_3 \cdot 3\text{THF}$ crystals are magnetically ordered at low temperature [$2(J+\frac{1}{2})$ gives the $(2J+1)$ typical Zeeman pattern], the 77 K spectra, $\text{Y}(\text{BH}_4)_3 \cdot 3\text{THF}$ mixed crystal spectra, and magnetic susceptibility measurements all strongly argue against this interpretation. One is left to conclude that the

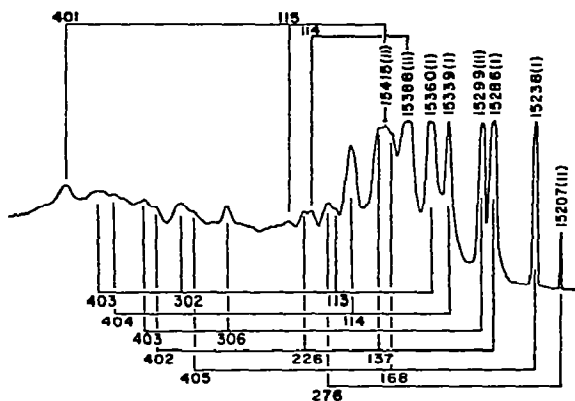


Fig. 4. Absorption spectrum of pure $\text{Er}(\text{BH}_4)_3 \cdot 3\text{THF } ^4\text{F}_{9/2}$ manifold at 1.6 K. Electronic origins are indicated by their transition frequency (cm^{-1}) and site system (I or II). Vibronic features (fundamental, overtone and combination bands) are assigned and are indicated by their separations from the origins (in cm^{-1}). For an estimation of their intensities, see table 4.

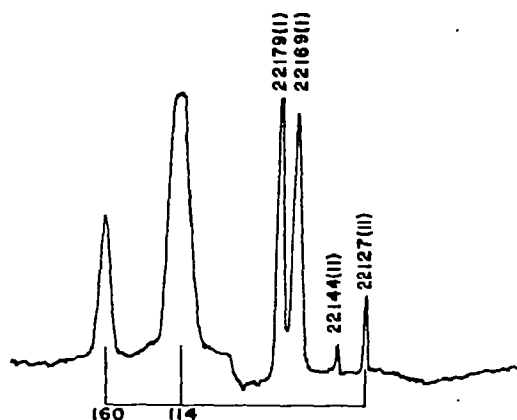


Fig. 6. Absorption spectrum of pure $\text{Er}(\text{BH}_4)_3 \cdot 3\text{THF } ^4\text{F}_{5/2}$ manifold at 1.6 K. Electronic origins are indicated by their transition frequency (cm^{-1}) and site system (I or II). Notice that 114 and 160 cm^{-1} vibronic features have large intensities relative to the origin.

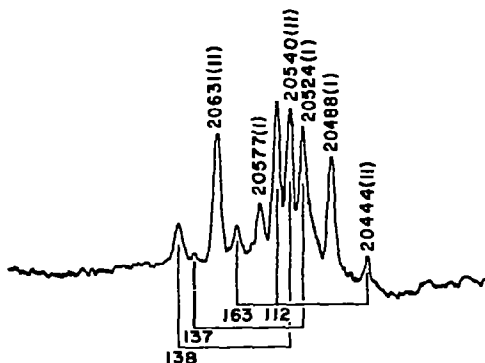


Fig. 5. Absorption spectrum of $\text{Er}^{3+}/\text{Gd}(\text{BH}_4)_3 \cdot 3\text{THF } ^4\text{F}_{7/2}$ manifold at 1.6 K. Electronic origins are indicated by their transition frequency (cm^{-1}) and site system (I or II). Note that vibronic features are often as intense as the origins.

such frequencies only slightly). It is just these motions which would be expected to couple best to electronic motion. Surprisingly, the intensity distribution found here is not dissimilar from that observed in $\text{U}(\text{BD}_4)_4/\text{HF}$, $\text{Zr}(\text{BD}_4)_4$ (compare ref. [18] with figs. 1–6 and table 5 of present work). Many manifolds have more than half of their total intensity in

vibronic transitions. Selected transitions are tabulated in table 5 according to J -manifold origin and progressions built on the origins. Most of the intensity is found in the first few members of a vibronic progression and usually within 400 cm^{-1} of the particular electronic origin.

A large vibronic intensity would be associated with covalently bonded systems and, in this regard, Gd, Er, $\text{Y}(\text{BH}_4)_3 \cdot 3\text{THF}$ are similar to $\text{U}(\text{BH}_4)_4$. However, large crystalfield splittings, as claimed for $\text{Er}(\text{cpd})_3$ [15], should also be expected. J -manifold splittings and centers of gravity for $\text{Er}(\text{BH}_4)_3 \cdot 3\text{THF}$ are presented in tables 4 and 6 and compared with other Er^{+3} compounds. Based upon these tabulations it is not possible to state that the crystal field is significantly different or larger for borohydrides than for other systems. In particular the $J = 3/2$ manifolds, if assumed to be pure, indicate small values of B_2^0 and B_2^2 . It is not at all clear why vibronic intensity seems to indicate covalent bonding character while the crystal field parameters and splittings seem to be in accord with standard ionic values. All that can be said is that for known covalent systems ($\text{U}(\text{BH}_4)_4$ [18] and XF_6 [26]) similar results are found. Apparently the crystal field is influenced greatly by the position of the protons even though it is of only medium strength.

Table 1

Summary of crystal field levels of neat $\text{Er}(\text{BH}_4)_3 \cdot 3\text{THF}$ and 5% $\text{Er}^{3+}/\text{La}(\text{BH}_4)_3 \cdot 3\text{THF}$ crystal. All electronic transitions reported for the pure crystal are also observed in mixed crystals of Y and $\text{Gd}(\text{BH}_4)_3 \cdot 3\text{THF}$ with the same transition frequency ($\pm 1.0 \text{ cm}^{-1}$) but different relative intensities. All data taken at 1.6 K

J-manifold and line group assignment a)		$\text{Er}(\text{BH}_4)_3 \cdot 3\text{THF}$		$5\% \text{Er}^{3+}/\text{La}(\text{BH}_4)_3 \cdot 3\text{THF}$			
		Vacuum corrected energy site I (cm^{-1})	f(b)	Vacuum corrected energy site II (cm^{-1})	f(b)	Vacuum corrected energy (cm^{-1})	f(b)
$^4I_{15/2}$	Z ₁	0		0		0	
	Z ₂	12		28		32	
	Z ₃	85				60	
	Z ₄					92	
$^4I_{9/2}$	B ₁	12359.4	1	12368.3	1	12440.3	1
	B ₂	12462.7	1	12690.1	2	12442.4	1
	B ₃	12583.1	2	12737.4	6	12510.0	1
	B ₄	12648.0	2			12547.7	1
	B ₅					12627.2	2
$^4F_{9/2}$	D ₁	15237.7	6	15206.6	1	15253.2	8
	D ₂	15286.4	7	15299.1	7	15281.9	2
	D ₃	15338.8	6	15387.8	8	15336.8	8
	D ₄	15359.9	7	15414.8	8	15353.1	6
	D ₅					15356.9	6
$^4S_{3/2}$	E ₁	18380.9	6	18452.8	7	18388.2	4
	E ₂	18399.7	6	18472.4	7	18423.7	4
$^2H_{11/2}$	F ₁	19069.9	6	19048.9	1	19056.8	8
	F ₂	19143.0	7	19108.0	1	19179.2	5
	F ₃	19164.8	9	19128.3	6	19185.9	8
	F ₄	19195.9	10			19202.4	7
	F ₅					19249.6	8
$^4F_{7/2}$	G ₁	20486.9	4	20444.2	1	20473.4	1
	G ₂	20523.9	5	20538.3	5	20509.4	5
	G ₃	20577.2	2	20631.9	5	20533.4	4
	G ₄					20564.0	4
$^4F_{5/2}$	H ₁	22169.1	5	22127.3	1	22174.3	1
	H ₂	22179.1	5	22144.5	1	22218.4	1
	H ₃					22231.9	1
$^4F_{3/2}$	I ₁	22533.1	2	22580.7	4	22553.7	1
	I ₂	22553.2	2	22602.6	3	22574.2	1
$^2H_{9/2}$	K ₁	24465.1	5	24481.2	5	24510.9	1
	K ₂	24510.4	1	24558.3	5	24537.5	5
	K ₃	24528.4	5	24752.8	5	24546.9	2
	K ₄			24782.0	6		
$^4G_{11/2}$	L ₁	26200.1	6	26158.2	1	26223.0	8
	L ₂	26295.2	9	26365.2	8	26358.5	10
	L ₃	26337.4	8	26397.9	9	26444.2	3
	L ₄	26438.4	10	26473.4	8	26484.9	7
	L ₅	26498.0	6	26543.0	2	26511.3	6
$^2G_{9/2}$	M ₁	27319.1	7	27281.8	1	27361.9	1
	M ₂	27374.5	8	27334.8	7	27370.3	4
	M ₃	27382.7	8	27355.7	2	27398.3	8
	M ₄	27401.0	1	27425.5	9	27416.3	2
	M ₅					27433.8	2

Table 1 (continued)

<i>J</i> -manifold and line group assignment ^{a)}	Er(BH ₄) ₃ ·3THF				5% Er ³⁺ /La(BH ₄) ₃ ·3THF				
	Vacuum corrected energy site I (cm ⁻¹)	<i>f</i> ^{b)}	Vacuum corrected energy site II (cm ⁻¹)	<i>f</i> ^{b)}	Vacuum corrected energy (cm ⁻¹)	<i>f</i> ^{b)}			
² K _{15/2} N ₁	27959	1	28013	1					
	N ₂	28085					4		
	N ₃	28120					5		
² G _{7/2} O ₁	28561.6	2	28407.4	1					
	O ₂	28606.0					2	28460.8	1
	O ₃							28527.4	2
² P _{3/2} P ₁	31476.0	1	31524.7	3					
	P ₂	31510.8					1	31561.5	3

a) See ref. [1] for conventions followed.

b) Relative intensity based on a 1 to 10 scale. These are very approximate numbers because the data are taken from a number of photographic plates and often on different samples.

Table 2

Vibrational frequencies of rare earth borohydrides (Er, Y, Gd) inferred from vibronic absorption spectra at 1.6 K

Frequency (cm ⁻¹)	Origin on which ν_j is observed	Samples for which ν_j is observed
ν_1 (114)	B ₁ (II), B ₃ (I), D ₃ (I), D ₄ (I), D ₃ (II), D ₄ (II), E ₁ (I), E ₂ (I), F ₁ (I), G ₁ (II), H ₁ (II), K ₁ (I), K ₁ (II), K ₃ (II), L ₁ (II), L ₃ (I), L ₅ (I), L ₅ (II), M ₁ (II), M ₁ (I), O ₂ (II), O ₁ (I), O ₂ (I)	Er(BH ₄) ₃ ·3THF
	F ₁ (I), F ₂ (II), G ₁ (II), H ₁ (II), K ₁ (II), L ₃ (I), L ₃ (II), M ₁ (II), M ₁ (I)	Er ³⁺ /Gd(BH ₄) ₃ ·3THF
	D ₁ (I), F ₁ (I), F ₂ (II), F ₃ (I), F ₄ (I), G ₁ (II), H ₁ (II), H ₂ (I), K ₁ (I), K ₁ (II), K ₂ (I), L ₁ (I), L ₂ (II), L ₄ (I), M ₁ (I), M ₂ (II)	Er ³⁺ /Y(BH ₄) ₃ ·3THF
ν_2 (138)	B ₂ (I), D ₂ (I), E ₂ (I), E ₁ (II), F ₁ (I), F ₃ (I), G ₂ (I), G ₂ (II), K ₁ (I), K ₂ (I), K ₃ (II), L ₄ (I), M ₁ (I), M ₂ (I), M ₃ (I), G ₂ (I)	Er(BH ₄) ₃ ·3THF
	F ₁ (I), F ₂ (II), F ₃ (II), G ₂ (I), G ₂ (II), K ₂ (I), L ₃ (I), M ₁ (I)	Er ³⁺ /Gd(BH ₄) ₃ ·3THF
	D ₂ (I), F ₂ (II), F ₃ (II), G ₂ (II), K ₂ (II), L ₃ (I)	Er ³⁺ /Y(BH ₄) ₃ ·3THF
ν_3 (163)	B ₁ (II), D ₁ (I), E ₁ (I), E ₁ (II), E ₂ (II), F ₃ (I), G ₁ (II), K ₁ (I), K ₃ (I), L ₄ (I), M ₁ (I), M ₃ (I), O ₂ (II)	Er(BH ₄) ₃ ·3THF
	D ₂ (I), F ₁ (I), F ₂ (II), F ₃ (I), G ₁ (II), H ₁ (II), K ₃ (I), L ₃ (I)	Er ³⁺ /Gd(BH ₄) ₃ ·3THF
	D ₂ (I), F ₁ (I), F ₃ (II), F ₃ (I), G ₁ (II), H ₁ (II), H ₂ (II), H ₂ (I), L ₃ (I), L ₄ (I)	Er ³⁺ /Y(BH ₄) ₃ ·3THF
ν_4 (402)	D ₂ (I), D ₂ (II), D ₃ (I), D ₄ (I), D ₄ (II), E ₁ (I), E ₂ (I), E ₁ (II), F ₁ (I), F ₂ (II), F ₃ (II), F ₃ (I), G ₁ (II), G ₁ (I), G ₂ (II), L ₂ (I), L ₃ (I), L ₃ (II), M ₁ (I), M ₂ (II), M ₃ (II), M ₃ (I), M ₄ (II)	Er(BH ₄) ₃ ·3THF
ν_5 (627)	E ₁ (I), E ₂ (I), F ₁ (I), F ₂ (II), F ₂ (I), F ₃ (I), F ₄ (I), L ₁ (I), L ₂ (I), L ₃ (I), L ₃ (II)	Er(BH ₄) ₃ ·3THF
ν_6 (713)	F ₃ (II), F ₂ (I), F ₄ (I), L ₂ (II), L ₃ (II), L ₄ (I), L ₄ (II)	Er(BH ₄) ₃ ·3THF
ν_7 (804)	G ₁ (II), G ₁ (I), G ₂ (II), L ₂ (I)	Er(BH ₄) ₃ ·3THF
ν_8 (994)	F ₁ (I), F ₃ (II), F ₂ (I), G ₁ (I), G ₂ (I), G ₂ (II), L ₁ (I)	Er(BH ₄) ₃ ·3THF
ν_9 (1081)	F ₁ (I), F ₂ (II), F ₃ (II), F ₂ (I), F ₃ (I), F ₄ (I), G ₁ (I), G ₂ (II)	Er(BH ₄) ₃ ·3THF

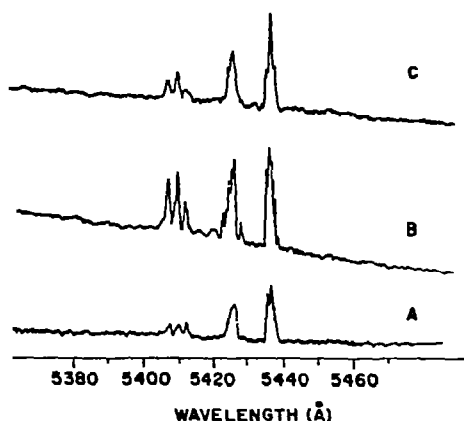


Fig. 7. Absorption spectra of $\text{Er}^{3+}/\text{La}(\text{BH}_4)_3 \cdot 3\text{THF } ^4\text{S}_{3/2}$ manifold at 1.6 K. (A), (B) and (C) are 1%, 5%, 20% samples, respectively. The two electronic transitions assigned are at 5437 Å (18388 cm^{-1}) and 5426 Å (18424 cm^{-1}). The weak sharp lines in the 5410 Å region, as well as those immediately in the vicinity of the origins, are satellite lines. Compare these spectra with those of fig. 1.

Coupling of low frequency vibrations to electronic motion is good.

In keeping with predicted small values of B_2^0 , $\text{Er}(\text{BH}_4)_3 \cdot 3\text{THF}$ shows no hypersensitivity [27] (tables 1 and 5) in the expected transitions ($^2\text{H}_{11/2}$, $^4\text{G}_{11/2} \leftarrow ^4\text{I}_{15/2}$, $\Delta J = 2$, $\Delta L = 2$).

4.2. $\text{Er}(\text{BH}_4)_3 \cdot 3\text{THF}/\text{La}(\text{BH}_4)_3 \cdot 3\text{THF}$ mixed crystals

Spectra of $\text{Er}(\text{BH}_4)_3 \cdot 3\text{THF}$ diluted (1%, 5%, 20%) into $\text{La}(\text{BH}_4)_3 \cdot 3\text{THF}$ are entirely different from those discussed above: the ($J+\frac{1}{2}$) rule is followed rigorously for the maximum number of observed lines; no vibronic intensity is found; and many sharp weak "satellite" features appear near electronic transitions (see table 1 and figs. 7 and 8). These spectra are much like the classical ionic rare earth spectra [1]. Based on these observations one can conclude: there is only one type of site in this crystal; bonding and/or coordination in $\text{La}(\text{BH}_4)_3 \cdot 3\text{THF}$ is different from that in the other compounds; and since the satellite intensity is proportional to the Er^{3+} concentration (not its square), it is due to defects caused by structural differences. This proportionality between the number of satellite lines, their intensity, and the Er^{3+} concentration is

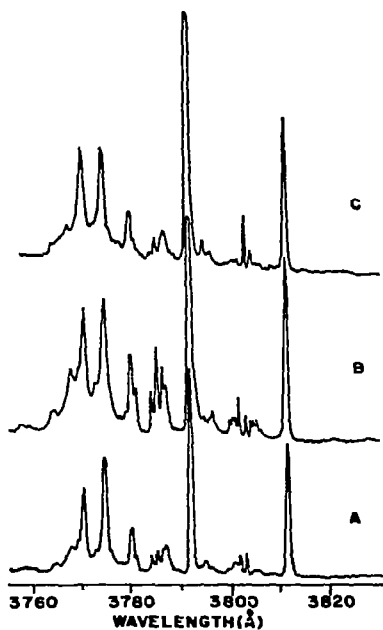


Fig. 8. Absorption spectra of $\text{Er}^{3+}/\text{La}(\text{BH}_4)_3 \cdot 3\text{THF } ^4\text{G}_{11/2}$ manifold at 1.6 K. (A), (B) and (C) are 1, 5, and 20 mole% mixed crystals, respectively. The five electronic transitions assigned are at 3812.4 Å (26223 cm^{-1}), 3792.8 Å (26358 cm^{-1}), 3780.5 Å (26444 cm^{-1}), 3774.7 Å (26485 cm^{-1}) and 3770.9 Å (26511 cm^{-1}). Weak sharp lines in the region 3795 to 3809 Å and 3782 to 3788 Å are satellite lines. The photographic plates show the numbers of lines more distinctly than do the tracings.

Table 3

$^4\text{I}_{15/2}$ ground manifold energy levels and vibrations observed in hot band spectra at 77 K (in cm^{-1})

$\text{Er}(\text{BH}_4)_3 \cdot 3\text{THF}$		$\text{Er}^{3+}/\text{La}(\text{BH}_4)_3 \cdot 3\text{THF}$
Site I	Site II	
0	0	0
12	28	32
85	120 a)	60
109 a)	130 b)	92
131 b)		
164 b)		

a) Observed also in room temperature Raman spectra.

b) The corresponding excited state vibrational frequencies inferred from electronic absorption spectra are 138 cm^{-1} and 163 cm^{-1} .

Table 4
Centers of gravity^{a)} of *J*-manifolds (in cm^{-1})

Sample	<i>LSJ</i> manifold label								
	⁴ I _{9/2}	⁴ F _{9/2}	⁴ S _{3/2}	² H _{11/2}	⁴ F _{7/2}	⁴ F _{5/2}	⁴ F _{3/2}	² H _{9/2}	⁴ G _{11/2}
Er(BH ₄) ₃ ·3THF									
site I	12514 ^{f)}	15316 ^{f)}	18390	19143 ^{f)}	20529 ^{f)}	22174 ^{f)}	22543	24501 ^{f)}	26442 ^{f)}
site II	12598 ^{f)}	15327 ^{f)}	18462	19095 ^{f)}	20538 ^{f)}	22136 ^{f)}	22592	24643 ^{f)}	26387 ^{f)}
Er ³⁺ /La(BH ₄) ₃ ·3THF	12513	15316	18406	19175 ^{f)}	20520	22209	22564	24532 ^{f)}	26404 ^{f)}
Er ³⁺ /LaCl ₃ b)	12460	15284	18399	19154 ^{f)}	20511 ^{f)}	22276	22507	24542	26379
Er E.S. c)	12504	15354	18474	19234	20605	22269	22608	24663	26495
Er ³⁺ /Y ₂ O ₃ d)	12490	15273	18274	19133	20470	22096	22410	24506	26276
Er(C ₅ H ₅) ₃ e)			18390 g)	18943 g)	20403 g)	21919 g)	22440	24305 ^{f)}	

a) Relative to the ground level of ⁴I_{15/2} manifold.

b) F. Varsanyi and G.H. Dieke, J. Chem. Phys. 36 (1962) 2951.

c) E.H. Erath, J. Chem. Phys. 34 (1961) 1985.

d) P. Kisliuk, W.F. Krupke and J.B. Gruber, J. Chem. Phys. 40 (1964) 3603.

e) See ref. [10].

f) Incomplete group.

g) The number of levels observed corresponds to a two sites structure.

not simple. For 1% and 20% mixed crystals, satellite line intensities are about equal ($\pm 25\%$) but for 5% Er³⁺/La(BH₄)₃·3THF, satellite intensity is about a factor of two greater than in the 1% or 20% sample. One can rationalize such variations based on forced creation of defect planes and major crystal faults at certain concentration levels which then allow heavier dopings without further structural discontinuities. There is also some ($\pm 20\%$) satellite intensity variation from crystal to crystal which can be attributed to crystal optical quality.

While the splitting patterns differ for La(BH₄)₃·3THF and Er, Gd, Y(BH₄)₃·3THF samples, the overall crystal field splittings and centers of gravity seem to be comparable. Tables 3, 4 and 6 give these comparisons.

4.3. Vibrational spectra and covalency

Perhaps the most meaningful determination of bonding character of Ln(BH₄)₃·3THF compounds is through comparison with similar compounds of generally agreed upon properties. The series Zr, Hf, U, Th(BH₄)₄, Al(BH₄)₃, and Na, KBH₄ represents a useful point of departure [16,18,19]. Solution infrared and crystal Raman spectra of Ln(BH₄)₃ have been

studied in the terminal and bridge hydrogen stretching regions (2000–2600 cm^{-1}). If a system is covalent with three hydrogen bridge bonds per borohydride group (Zr, Hf, U, Th(BH₄)₄) this region shows one peak at ca. 2600 cm^{-1} and 2 at ca. 2200 cm^{-1} ; if a system is covalent with 2 hydrogen bridge bonds per borohydride group [Al(BH₄)₃ and solid Th, U(BH₄)₄] this region shows 2 peaks at ca. 2600 cm^{-1} and 2 peaks at ca. 2200 cm^{-1} ; and if a system is ionic (BH₄ hydrogens equivalent like Na, KBH₄) this spectral region gives a single broad featureless peak. Rare earth borohydrides show a single peak at 2450 cm^{-1} and a doublet at 2185 and 2225 cm^{-1} , all three of which are rather broad. This indicates a much more covalent structure than Na, KBH₄ and a slightly less covalent structure than Th(BH₄)₄.

Based on this rather weak vibrational evidence, and low vapor pressure, one would expect a polymeric or site-bridging structure in the solid, as is found in Th, U, Np(BH₄)₄, with mixed double- and triple-hydrogen bridge bonded borohydride groups. The double bonded BH₄ groups would bridge two sites and the triple bonded BH₄ groups would be one-site terminal groups [17].

Table 5
Relative intensities of selected vibronic features of pure crystal $\text{Er}(\text{BH}_4)_3 \cdot 3\text{THF}$ at 1.6 K

<i>LSJ</i> manifold label	Vacuum corrected frequency (cm^{-1})	Assignment a)	Relative b) intensity	<i>LSJ</i> manifold label	Vacuum corrected frequency (cm^{-1})	Assignment a)	Relative b) intensity	
$^4\text{I}_{9/2}$	12368.3	origin $\text{B}_1(\text{II})$	10		19008.4	$\text{E}_1(\text{I})+\nu_5$	1	
	12482.4	$\text{B}_1(\text{II})+\nu_1$	10		18399.7	origin $\text{E}_2(\text{I})$	10	
	12530.4	$\text{B}_1(\text{II})+\nu_3$	5		18511.0	$\text{E}_2(\text{I})+\nu_1$	1	
	12462.7	origin $\text{B}_2(\text{I})$	10		18536.7	$\text{E}_2(\text{I})+\nu_2$	<1	
	12601.5	$\text{B}_2(\text{I})+\nu_2$	5		18625.8	$\text{E}_2(\text{I})+2 \times \nu_1$	2	
	1258.1	origin $\text{B}_3(\text{I})$	10		18673.1	$\text{E}_2(\text{I})+\nu_1+\nu_3$	1	
	12699.4	$\text{B}_3(\text{I})+\nu_1$	2		18707.4	$\text{E}_2(\text{I})+\nu_2+\nu_3$	1	
					18804.5	$\text{E}_2(\text{I})+\nu_4$	3	
$^4\text{F}_{9/2}$	15206.6	origin $\text{D}_1(\text{II})$	10		19026.4	$\text{E}_2(\text{I})+\nu_5$	1	
	15482.6	$\text{D}_1(\text{II})+\nu_1+\nu_3$	10		18452.8	origin $\text{E}_1(\text{II})$	10	
	15237.7	origin $\text{D}_1(\text{I})$	10		18592.2	$\text{E}_1(\text{II})+\nu_2$	2	
	15405.5	$\text{D}_1(\text{I})+\nu_2$	8		18617.8	$\text{E}_1(\text{II})+\nu_3$	1	
	15642.7	$\text{D}_1(\text{I})+\nu_4$	1		18759.0	$\text{E}_1(\text{II})+\nu_2+\nu_3$	1	
	15286.4	origin $\text{D}_2(\text{I})$	10		18858.0	$\text{E}_1(\text{II})+\nu_4$	1	
	15423.0	$\text{D}_2(\text{I})+\nu_2$	8					
	15512.2	$\text{D}_2(\text{I})+2 \times \nu_1$	1		$^4\text{F}_{5/2}$	22127.3	origin $\text{H}_1(\text{II})$	10
	15688.3	$\text{D}_2(\text{I})+\nu_4$	1			22241.4	$\text{H}_1(\text{II})+\nu_1$	200
	15299.1	origin $\text{D}_2(\text{II})$	10			22287.4	$\text{H}_1(\text{II})+\nu_3$	50
	15605.6	$\text{D}_2(\text{II})+\nu_2+\nu_3$	1		$^2\text{H}_{9/2}$	24465.1	origin $\text{K}_1(\text{I})$	10
	15702.1	$\text{D}_2(\text{II})+\nu_4$	1			24579.6	$\text{K}_1(\text{I})+\nu_1$	1
	15338.8	origin $\text{D}_3(\text{I})$	10			24605.6	$\text{K}_1(\text{I})+\nu_2$	1
	15453.3	$\text{D}_3(\text{I})+\nu_1$	8			24627.7	$\text{K}_1(\text{I})+\nu_3$	3
	15743.2	$\text{D}_3(\text{I})+\nu_4$	1			24741.7	$\text{K}_1(\text{I})+\nu_1+\nu_3$	1
	15359.9	origin $\text{D}_4(\text{I})$	10			24907.0	$\text{K}_1(\text{I})+\nu_1+2 \times \nu_3$	<1
	15473.0	$\text{D}_4(\text{I})+\nu_1$	1			24481.2	origin $\text{K}_1(\text{II})$	10
	15662.3	$\text{D}_4(\text{I})+\nu_2+\nu_3$	2			24594.0	$\text{K}_1(\text{II})+\nu_1$	3
15762.8	$\text{D}_4(\text{I})+\nu_4$	2			24709.9	$\text{K}_1(\text{II})+2 \times \nu_1$	<1	
15387.8	origin $\text{D}_3(\text{II})$	10			24937.4	$\text{K}_1(\text{II})+\nu_1+2 \times \nu_3$	<1	
15501.8	$\text{D}_3(\text{II})+\nu_1$	1			24510.4	origin $\text{K}_2(\text{I})$	10	
15414.8	origin $\text{D}_4(\text{II})$	10			24648.9	$\text{K}_2(\text{I})+\nu_2$	10	
15529.7	$\text{D}_4(\text{II})+\nu_1$	1			24528.4	origin $\text{K}_3(\text{I})$	10	
15815.6	$\text{D}_4(\text{II})+\nu_4$	2			24694.3	$\text{K}_3(\text{I})+\nu_3$	2	
$^4\text{S}_{3/2}$	18380.9	origin $\text{E}_1(\text{I})$	10		24828.4	$\text{K}_3(\text{I})+\nu_2+\nu_3$	<1	
	18494.9	$\text{E}_1(\text{I})+\nu_1$	1		24752.8	origin $\text{K}_3(\text{II})$	10	
	18549.4	$\text{E}_1(\text{I})+\nu_3$	<1		24868.8	$\text{K}_3(\text{II})+\nu_2$	1	
	18654.7	$\text{E}_1(\text{I})+\nu_1+\nu_3$	1		24892.1	$\text{K}_3(\text{II})+\nu_1$	1	
	18686.0	$\text{E}_1(\text{I})+\nu_2+\nu_3$	1		24981.7	$\text{K}_3(\text{II})+2 \times \nu_1$	<1	
	18782.0	$\text{E}_1(\text{I})+\nu_4$	2		24782.0	origin $\text{K}_4(\text{II})$	10	
					24952.4	$\text{K}_4(\text{II})+\nu_3$	<1	

a) See table 2 for numbering of vibrations.

b) Relative intensities are much better within a given manifold than between manifolds. They are probably at best good to roughly 10%.

Table 6
Overall splitting of *J*-manifolds and comparison with Er³⁺/LaCl₃ and Er³⁺/Y₂O₃ at 1.6 K

LSJ manifold label	Overall splittings (cm ⁻¹)				
	Er(BH ₄) ₃ ·3THF		Er ³⁺ /La(BH ₄) ₃ ·3THF	Er ³⁺ /LaCl ₃ a)	Er ³⁺ /Y ₂ O ₃ b)
	Set I	Set II			
⁴ I _{9/2}	289 c)	369 c)	187	155	280
⁴ F _{9/2}	122 c)	218 c)	104	65	316
⁴ S _{3/2}	19	20	35	24	88
⁴ H _{11/2}	126	79 c)	193 c)	43 c)	214
⁴ F _{7/2}	37 c)	188 c)	91	71 c)	229
⁴ F _{5/2}	10 c)	160 c)	58	16	126
⁴ F _{3/2}	20	22	20	30	166
² H _{9/2}	63 c)	301 c)	36 c)	100	244
⁴ G _{11/2}	298 c)	385 c)	290 c)	139	368
² G _{9/2}	82 c)	144 c)	72	24 c)	

a) F. Varsanyi and G.H. Dieke, J. Chem. Phys. 36 (1962) 2951.

b) P. Kisliuk, W.F. Krupke and J.B. Gruber, J. Chem. Phys. 40 (1964) 3606.

c) Incomplete group, total splitting of known levels is given.

Table 7
Ionic radii of various ions of interest [source: Handbook of Physics and Chemistry, 50th Ed. (CRC Press, Cleveland, Ohio, 1970) F152]

	Ion									
	Sc ³⁺	Y ³⁺	La ³⁺	Sm ³⁺	Gd ³⁺	Er ³⁺	Zr ⁴⁺	Hf ⁴⁺	Th ⁴⁺	U ⁴⁺
Radius (in Å)	0.732	0.893	1.016	0.964	0.938	0.881	0.79	0.78	1.02	0.97

4.4. Structure differences

It is initially quite surprising to find a structure difference across the lanthanide series for compounds with such complex ligands (BH₄ and C₄H₈O). The only other compound for which a change in structure is known is LnCl₃. A structural change has been noted, however, for Sc(cpd)₃ and Sm(cpd)₃ [4,6]. The ionic radii for pertinent ions are given in table 7. The cause of this structure variation is most likely associated with size relationships (La³⁺ is much larger than Gd³⁺, Er³⁺, Y³⁺ which are all about the same size), but why for borohydrides and not, for example, hydrated chlorides or ethyl sulfates, or double nitrates, etc., is not obvious. A fuller discussion of this point must

await the more complete crystal study. In this regard, the synthesis and structure determination of Sc(BH₄)₃ would be quite interesting.

As mentioned above, it was not possible to grow crystals from diethyl ether or MeTHF. It appears that THF is an essential feature of both structures and that THF packing, interfered with or prevented by the bulkier methyl groups, is an important consideration for both crystal configurations.

An additional useful tool for understanding structure and bonding in these systems will be magnetic resonance since both ions and ligands possess nuclear moments. Such studies are commencing presently in our laboratory.

References

- [1] a. G.H. Dieke, *Spectra and Energy Levels of Rare Earth Ions in Crystals* (Interscience, New York, 1968).
 b. B.G. Wybourne, *Spectroscopic Properties of Rare Earths* (Interscience, New York, 1965); *J. Chem. Phys.* **34** (1961) 279.
 c. A. Abragam and B. Bleaney, *Electron Paramagnetic Resonance of Transition Ions* (Oxford Univ. Press, London, 1970).
- [2] a. H. Gysling and M. Tsutsui, *Adv. Organometal. Chem.* **9** (1970) 361.
 b. R.G. Hayes and J.L. Thomas, *Organometal. Chem. Rev.* **A7** (1971) 1.
 c. B. Kanellakopulos and K.W. Bagnall, in: H.J. Emeléus and K.W. Bagnell, eds., *MTP International Review of Science, Inorganic Chem. Series One, Vol. 7* (Univ. Park Press, Baltimore, Md., 1972) p. 299.
 d. J.D. Jamerson, A.P. Masino and J. Takats, *J. Organometal. Chem.* **65** (1974) C33.
- [3] J.L. Atwood, J.H. Burns and P.G. Laubereau, *ONRL-4706 Chem. Rev. Ann. Rept.* (1971) p. 77.
- [4] J.L. Atwood and K.D. Smith, *J. Am. Chem. Soc.* **95** (1973) 1488; *Chem. Comm.* (1972) 593.
- [5] J.L. Atwood, J.H. Burns and P.G. Laubereau, *J. Am. Chem. Soc.* **95** (1973) 1830.
- [6] L.H. Wong, T.Y. Lee and Y.T. Lee, *Acta Cryst.* **B25** (1969) 2580.
- [7] J. de Villiers and J.C.A. Boeyens, *Acta Cryst.* **B28** (1972) 2335.
- [8] L.J. Nugent, P.G. Laubereau, G.K. Werner and K.L. Vander Sluis, *J. Organometal. Chem.* **27** (1971) 365.
- [9] F. Calderazzo, R. Pappalardo and S. Losi, *J. Inorg. Nuc. Chem.* **28** (1966) 987.
- [10] R. Pappalardo, *Helv. Phys. Acta* **38** (1965) 178; *J. Mol. Spectry.* **29** (1969) 13; *J. Chem. Phys.* **49** (1968) 1545.
- [11] R. Pappalardo and S. Losi, *J. Inorg. Nuc. Chem.* **27** (1965) 733.
- [12] R.D. Fischer and H. Fischer, *J. Organometal. Chem.* **8** (1967) 155.
- [13] E.O. Fischer and H. Fischer, *J. Organometal. Chem.* **3** (1965) 181.
- [14] R. Pappalardo and C.K. Jørgensen, *J. Chem. Phys.* **46** (1967) 632.
- [15] The large crystal field splitting reported for $\text{Er}(\text{cpd})_3$ is somewhat questionable due to the possibility of two crystallographically inequivalent sites, like $\text{Sm}(\text{cpd})_3$, and remaining hot band intensity. In fact, the number of observed lines for different manifolds is not inconsistent with a two-site hypothesis.
- [16] B.D. James and M.G.H. Wallbridge, *Proc. Inorg. Chem.* **11** (1970) 99.
- [17] a. E.R. Bernstein, T.A. Keiderling, S.J. Lippard and J.J. Mayerle, *J. Am. Chem. Soc.* **94** (1972) 2552.
 b. E.R. Bernstein, W.C. Hamilton, T.A. Keiderling, S.J. La Placa, S.J. Lippard and J.J. Mayerle, *Inorg. Chem.* **11** (1972) 3009.
- [18] E.R. Bernstein and T.A. Keiderling, *J. Chem. Phys.* **59** (1973) 2105 and references therein.
- [19] a. T.A. Keiderling, W.T. Wozniak, R.S. Gay, D. Jurkowitz, E.R. Bernstein, S.J. Lippard and T.G. Spiro, *Inorg. Chem.* **14** (1975) 576; references to early works are cited therein.
 b. V.V. Volkov, K.G. Myakishev and Z.A. Grankina, *Russ. J. Inorg. Chem.* **15** (1970) 1490.
 c. B.D. James, B.E. Smith and M.G.H. Wallbridge, *J. Mol. Struct.* **14** (1972) 327.
 d. B.E. Smith and B.D. James, *Inorg. Nucl. Chem. Letters* **7** (1971) 857.
 e. N. Davies, M.G.H. Wallbridge, B.E. Smith and B.D. James, *JCS. Dalton* (1973) 162.
 f. J.J. Marks, W.J. Kennelly, J.R. Kolb and L.A. Shimp, *Inorg. Chem.* **11** (1972) 2540.
- [20] E.R. Bernstein and K.M. Chen, unpublished results.
- [21] B. Segal, K.M. Chen, E.R. Bernstein and S.J. Lippard, unpublished results.
- [22] a. O. Klejnot, Dissertation, University of Munich (1955).
 b. E. Zange, *Chem. Ber.* **93** (1960) 652.
- [23] a. H.I. Schlessinger, H.C. Brown and E.K. Hyde, *J. Am. Chem. Soc.* **75** (1953) 209.
 b. D.C. Bradley and M.M. Faktor, *Chem. and Ind. (London)* (1958) 1332.
 c. M.D. Taylor and C.P. Carter, *J. Inorg. Nucl. Chem.* **24** (1962) 387.
- [24] K.M. Chen, Thesis, Princeton University (1975); also University Microfilms INC. Ann Arbor, Michigan.
- [25] See for example F.J. DiSalvo et al., *J. Chem. Phys.* **62** (1975) 2575, and references therein.
- [26] a. E.R. Bernstein and G.R. Meredith, *J. Chem. Phys.*, submitted for publication.
 b. E.R. Bernstein and J.D. Webb, unpublished results.
- [27] a. C.K. Jørgensen and B.R. Judd, *Mol. Phys.* **8** (1964) 281.
 b. B.R. Judd, *Phys. Rev.* **127** (1962) 750, and: *Operator Techniques in Atomic Spectroscopy* (McGraw-Hill, New York, 1963).
 c. G.S. Ofelt, *J. Chem. Phys.* **37** (1962) 511.